

Superconductivity in Ca-intercalated epitaxial graphene on silicon carbide

Kang Li, Xiao Feng, Wenhao Zhang, Yunbo Ou, Lianlian Chen et al.

Citation: *Appl. Phys. Lett.* **103**, 062601 (2013); doi: 10.1063/1.4817781

View online: <http://dx.doi.org/10.1063/1.4817781>

View Table of Contents: <http://apl.aip.org/resource/1/APPLAB/v103/i6>

Published by the [AIP Publishing LLC](#).

Additional information on *Appl. Phys. Lett.*

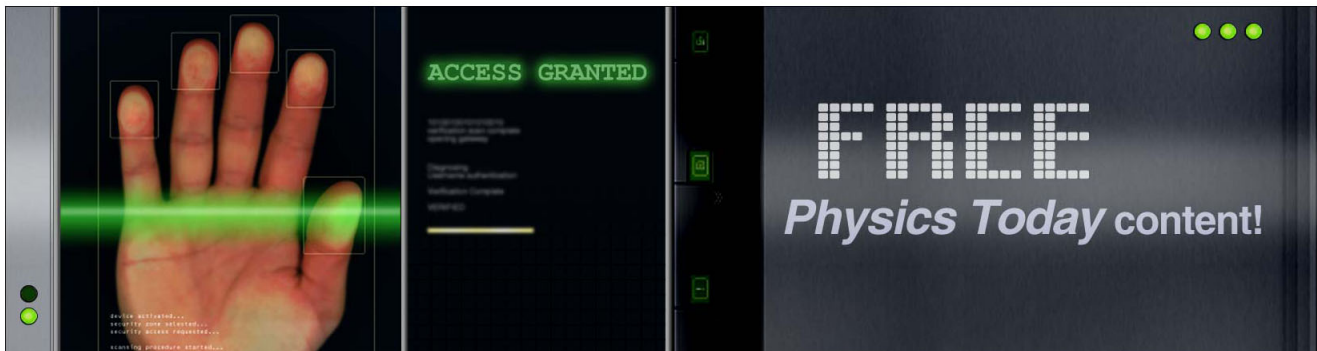
Journal Homepage: <http://apl.aip.org/>

Journal Information: http://apl.aip.org/about/about_the_journal

Top downloads: http://apl.aip.org/features/most_downloaded

Information for Authors: <http://apl.aip.org/authors>

ADVERTISEMENT



Superconductivity in Ca-intercalated epitaxial graphene on silicon carbide

Kang Li,¹ Xiao Feng,^{1,2} Wenhao Zhang,^{1,2} Yunbo Ou,¹ Lianlian Chen,¹ Ke He,^{1,a)} Li-Li Wang,¹ Liwei Guo,¹ Guodong Liu,¹ Qi-Kun Xue,² and Xucun Ma^{1,a)}

¹Beijing National Laboratory for Condensed Matter Physics & Institute of Physics, Chinese Academy of Sciences, Beijing 100190, China

²State Key Laboratory of Low-Dimensional Quantum Physics, Department of Physics, Tsinghua University, Beijing 100084, China

(Received 4 July 2013; accepted 22 July 2013; published online 5 August 2013)

We have prepared Ca-intercalated multilayer epitaxial graphene films on silicon carbide and observed superconductivity in them with both magnetic and transport measurements. Superconducting transition has been detected at temperature up to 7 K in Ca-intercalated epitaxial graphene with the thickness down to 10 layers grown on both Si-face and C-face of silicon carbide. The result demonstrates intercalated epitaxial graphene as a good platform to study graphene-based superconductivity. © 2013 AIP Publishing LLC. [<http://dx.doi.org/10.1063/1.4817781>]

Carbon allotropes have been attracting continuous research interests from the field of superconductivity because they are believed to be potential superconductors with high transition temperatures (T_c) when supplied with additional charge carriers.¹ Superconductivity has been experimentally observed not only in bulk carbon materials, such as diamond and graphite, but also in carbon nano-structures, such as full-erene and carbon nanotube, that are doped with certain impurities.^{2–5} What is particularly interesting among them is graphite intercalation compounds (GICs).⁶ In this class of materials, dopants reside between carbon sheets of graphite, usually in ordered way, which makes their structure relatively well-defined and their physical properties, thus easy to be studied.⁶ Superconductive GICs were first found decades ago in KC_8 but with T_c well below 1 K.² The recent discoveries of GICs with much higher T_c , CaC_6 (11.5 K) and YbC_6 (6.5 K), reactivate the researches in this direction.⁷ Graphene is a two-dimensional (2D) version of graphite exhibiting novel electronic structure and properties.^{8,9} It is very intriguing to see how the superconductivity in GICs evolves in the 2D limit. Superconductivity in doped graphene down to single layer has been investigated theoretically,^{10–13} with unique properties, for example, chiral superconductivity,¹¹ predicted. A recent work reported the observation of superconductivity in potassium-doped graphene flakes.¹⁴ However, the small crystallite size and non-uniformity in macroscopic scale, which are unavoidable for flake samples, make systematic studies of their structures and superconductivity rather challenging. Epitaxial graphene (EG), especially that grown on insulating silicon carbide (SiC) substrate, can be made uniform and single crystalline in macroscopic size,⁹ which provides a much better system to fabricate superconductive intercalated graphene.

EG films can be grown on both the (0001) (Si face) and (000 $\bar{1}$) (C-face) surfaces of SiC substrates by thermal decomposition of SiC and sublimation of Si atoms, but the structures of the EG on the two surfaces are different.¹⁵ In the EG on Si-face of SiC, carbon monolayers stack in the

same way as in bulk graphite (AB-stacking).¹⁶ On the other hand, for EG on C-face, there are rotational faults between adjacent carbon monolayers, which decouple their electrons so that the sample exhibits properties analogous to a single layer graphene.¹⁷ In this work, with the conventional method of synthesizing CaC_6 from bulk graphite,¹⁸ we prepared Ca-intercalated multilayer EG on both Si- and C-faces of SiC, and realized superconductivity in both cases.

We use commercial SiC substrates to grow EG films. The preparation consists of the typical hydrogen etching and graphitization processes.⁹ Figures 1(a) and 1(b) display the typical atomic force microscope (AFM) images of the resulting EGs on C- and Si-faces of SiC, respectively. Both images show clear step-terrace structure with atomically flat terraces, reflecting the morphology of the below SiC substrates. The white linear features in Fig. 1(a) are ridge structures resulting from compressive strain, which are often seen on the surfaces of EG on SiC.¹⁹ Raman spectroscopy is a common technique to characterize graphene.^{20,21} Figure 1(c) shows the Raman spectra of three representative EG samples that were used for intercalation reaction and superconductivity measurements: one grown on Si-face and the other two on C-face of SiC. In all the three spectra, the most prominent features are located at $\sim 1580\text{ cm}^{-1}$ and $\sim 2700\text{ cm}^{-1}$, which are the characteristic G and $2D$ peaks of graphite/graphene, respectively. This observation confirms the existence of graphene layers on the SiC substrates. The low intensity of D peaks at $\sim 1350\text{ cm}^{-1}$, which corresponds to zone-boundary phonons, suggests low defect density and high quality of the samples.^{20,21} The several small features around G peaks come from SiC substrates. The thickness of EG on SiC can be estimated from intensity ratio between the peaks of SiC and graphene, as well as the width of $2D$ peak.²¹ The thickness of the EG sample on Si-face of SiC is estimated to be ~ 10 layers (L). The two samples on C-face have thicknesses of ~ 10 L and ~ 50 L, respectively.

The procedure of intercalation reaction is basically the same as that used for preparation of bulk CaC_6 .¹⁸ The EG covered SiC substrates are immersed into melted Li-Ca alloy, with the Li:Ca molar ratio of 3, which is contained in a tantalum crucible. The crucible is then vacuum-sealed in a

^{a)}Authors to whom correspondence should be addressed. Electronic addresses: kehe@aphy.iphy.ac.cn and xcma@aphy.iphy.ac.cn

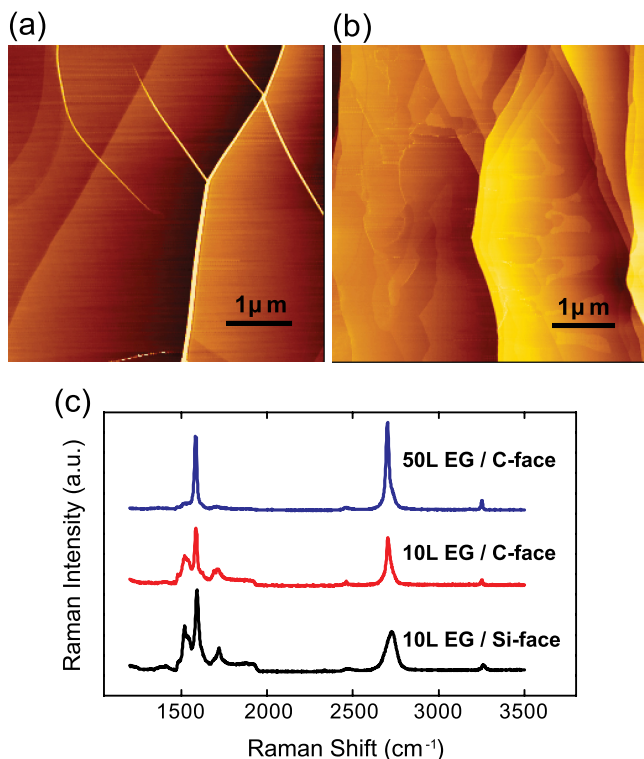


FIG. 1. (a) and (b) AFM images ($5 \mu\text{m} \times 5 \mu\text{m}$) of the surface morphology of EG films grown on the C-face (a) and Si-face of SiC (b). (c) Raman spectra of the three EG samples on SiC used for intercalation reaction: 50 L EG on C-face of SiC (blue), 10 L EG on C-face SiC (red), and 10 L EG on Si-face SiC (black).

quartz tube and heated at 350°C for 7 days for intercalation reaction. The role of Li is twofold: first, it lowers the melting temperature of Ca; second, it acts as the precursor for intercalation of Ca into graphene.¹⁸ With enough long reaction time, Li atoms that enter between carbon layers in advance can be completely substituted by Ca atoms and expelled out of graphene.¹⁸ After intercalation reaction, the samples are taken for superconductivity measurements soon after being extracted from the remaining Li-Ca metal. The sample handlings are carried out in an argon glove-box to avoid ambient oxidation of the samples and Li-Ca alloy. Superconducting properties are investigated by both magnetic and transport measurements with a vibration sample magnetometer (VSM) and a Physical Property Measurement System (PPMS) of Quantum Design, Inc., respectively.

It is to note that since the superconductivity of CaC_6 is very vulnerable to ambient conditions,⁷ a Ca-intercalated EG sample loses its superconductivity in very short time (less than 1 min) in atmosphere. Nevertheless, Ca-intercalated EG samples always have residual Li-Ca metal on their surfaces, which can protect the samples from deterioration for several hours. The metallic overlayer however introduces paramagnetic background and parallel conduction channels in magnetic and transport measurements, respectively, which can cover the superconducting signal. Thus, superconductivity could only be measured in samples covered with medium amount of residual metals.

Figure 2(a) shows the field cooling (FC) (red) and zero-field cooling (ZFC) (black) curves of temperature (T) dependent magnetic moment (m) of the intercalated EG sample

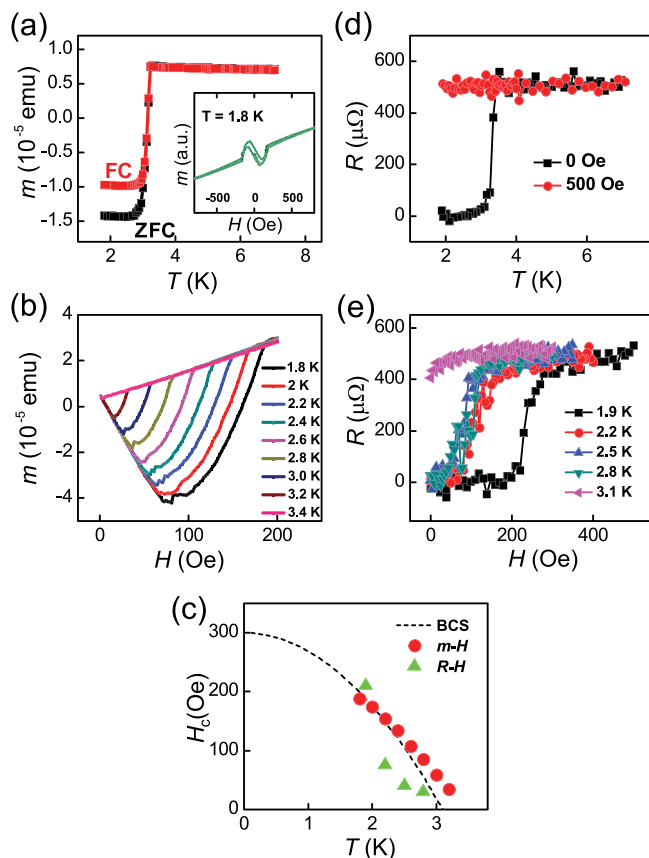


FIG. 2. Characterization of superconductivity in the intercalated EG sample of ~ 50 L on the C-face of SiC. (a) Field-cooling (FC) ($H = 30$ Oe) (red) and zero-field-cooling (ZFC) (black) $m(T)$ plots. Inset: magnetization hysteresis loop obtained at 1.8 K. (b) $m(H)$ plots at different temperatures. (c) H_c - T phase diagram determined from $m(H)$ (solid red circles) and $R(H)$ (solid green triangles) data. The black dashed line is a fit to the BCS theory $H_c(T) = H_c(0)[1 - (T/T_c)^2]$. (d) $R(T)$ plots measured at zero field (black) and $H = 500$ Oe (red). (e) $R(H)$ plots at different temperatures.

of ~ 50 L on C-face of SiC measured with VSM. At high temperature, m is positive and shows little temperature dependence, indicating a paramagnetic behavior. At 3.2 K, there is a sudden drop of the measured magnetic moment from positive to negative in both the FC and ZFC curves, with the latter one exhibiting larger magnitude of change. The magnetic field (H) dependent m measured at 1.8 K is shown in the inset of Fig. 2(a), which is clearly a superimposition of a paramagnetic part and a diamagnetic one at low field. The strong diamagnetic signal at low temperature and low magnetic field suggests superconductivity in the sample, whereas the paramagnetic signal can be mainly attributed to the residual Li-Ca metal on the sample surface. The superconductivity is further demonstrated by a series of m - H curves measured at different temperatures (see Fig. 2(b)). These curves exhibit the same negative initial susceptibility (m/H) (forming a downward straight-line) indicating superconducting phase. Depending on the temperature, they then jump to positive values at different magnetic fields, and finally merge into one upward straight-line (the paramagnetic background). It is the typical behavior of Meissner effect. The critical fields (H_c) at different temperatures are obtained from the positions where the curves join the straight-line of paramagnetic background, which are plotted in Fig. 2(c) (solid red circles). The H_c - T relation cannot be well fitted with the BCS theory (the

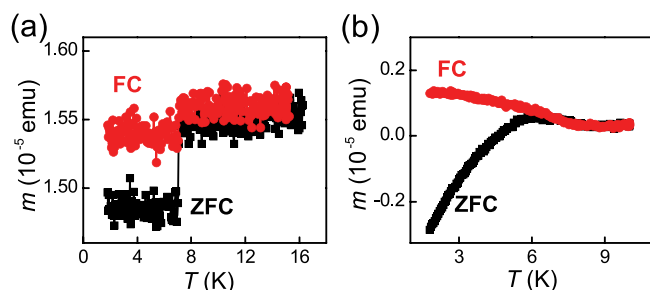


FIG. 3. Characterization of superconductivity in the intercalated EG samples of ~ 10 L. (a) FC ($H = 30$ Oe) (red) and ZFC (black) $m(T)$ plots of the intercalated EG on the Si-face of SiC. (b) FC ($H = 30$ Oe) (red) and ZFC (black) $m(T)$ plots measured at $H = 30$ Oe on the C-face of SiC.

black dashed curve in Fig. 2(c)), but shows the similar tendency with that of bulk CaC_6 .¹⁸ Compared with bulk CaC_6 , the H_c values of the intercalated EG are smaller by one order of magnitude. We have carried out control experiment with bare SiC substrates that are heated in melted Li-Ca alloy under the same condition as that for preparing the intercalated EG. No indication of any superconductivity transition could be found. Thus, the observed superconductivity can only be attributed to the intercalated EG.

Figure 2(d) displays temperature dependent resistance of an intercalated EG sample of ~ 50 L on C-face of SiC. At zero field, an abrupt drop of resistance to near zero is observed at ~ 3.4 K, suggesting a superconducting transition (black). The superconductivity is further confirmed by quench of the transition by a magnetic field of 500 Oe (red). Figure 2(e) exhibits the field dependent resistance at various temperatures from which we can also obtain the temperature dependence of H_c . The H_c - T relation (solid green triangles in Fig. 2(c)) is basically consistent with the data obtained from magnetic measurements. Thus, superconductivity in the Ca-intercalated EG of 50 L on C-face of SiC is unambiguously confirmed by both magnetic and transport measurements.

Signature of superconducting transition is also observed in thinner Ca-intercalated EGs (down to 10 L) not only grown on C-face, but also on Si-face SiC. Figure 3(a) shows the FC and ZFC m - T curves of a Ca-intercalated EG of ~ 10 L on Si-face of SiC. The curves show a clear drop below 7 K, implying a superconducting transition here. However, the amplitude of the drop is very small, only around 5×10^{-7} emu, which suggests that only a small portion of the sample is superconductive. In a Ca-intercalated EG of ~ 10 L on C-face of SiC, distinct deviation between FC and ZFC curves is observed below 7 K (Fig. 3(b)). The measured magnetic moment gradually decreases in the ZFC curve, suggesting non-uniform superconductivity, probably resulting from sample deterioration under ambient condition as usually seen in bulk CaC_6 .

Due to the weaker signal and increased fragility of the samples, as well as the not-well-controlled capping layer of residual metal, it is difficult to obtain well-repeated

superconductivity in intercalated EGs as thin as 10 L. The temperature and sharpness of superconducting transition differ from samples to samples, which prevents us from obtaining reliable thickness dependent data of the superconductivity and observing superconductivity in thinner samples. Better sample protection methods are crucial for further in-depth studies. Nevertheless, the results so far have demonstrated that superconductivity can indeed be realized in EGs through intercalation reaction with the same method for synthesizing GICs. The large crystalline size and well-controlled thickness of EG samples make the electronic structure and superconductivity of their intercalation compounds easy to be studied by many characterization techniques, which open a gate to systematic experimental investigations on graphene-based superconducting phenomena.

This work was supported by National Science Foundation (Grant No. 91021006) and the Ministry of Science and Technology of China (Grant No. 2012CB921302), and the Chinese Academy of Sciences.

- ¹X. Blase, E. Bustarret, C. Chapelier, T. Klein, and C. Marcenat, *Nature Mater.* **8**, 375 (2009).
- ²N. B. Hannay, T. H. Geballe, B. T. Matthias, K. Andres, P. Schmidt, and D. MacNair, *Phys. Rev. Lett.* **14**, 225 (1965).
- ³M. Kociak, A. Yu. Kasumov, S. Gueron, B. Reulet, I. I. Khodos, Yu. B. Gorbatov, V. T. Volkov, L. Vaccarini, and H. Bouchiat, *Phys. Rev. Lett.* **86**, 2416 (2001).
- ⁴A. Y. Ganin, Y. Takabayashi, Y. Z. Khimyak, S. Margadonna, A. Tamai, M. J. Rosseinsky, and K. Prassides, *Nature Mater.* **7**, 367 (2008).
- ⁵E. A. Ekimov, V. A. Sidorov, E. D. Bauer, N. N. Mel'nik, N. J. Curro, J. D. Thompson, and S. M. Stishov, *Nature* **428**, 542 (2004).
- ⁶M. S. Dresselhaus and G. Dresselhaus, *Adv. Phys.* **51**, 1 (2002).
- ⁷T. E. Well, M. Ellerby, S. S. Saxena, R. P. Smith, and N. T. Skipper, *Nat. Phys.* **1**, 39 (2005).
- ⁸A. H. Geim, *Science* **324**, 1530 (2009).
- ⁹K. V. Emtsev, A. Bostwick, K. Horn, J. Jobst, G. L. Kellogg, L. Ley, J. L. McChesney, T. Ohta, S. A. Reshanov, J. Röhrl, E. Rotenberg, A. K. Schmid, D. Waldmann, H. B. Weber, and Th. Seyller, *Nature Mater.* **8**, 203 (2009).
- ¹⁰G. Profeta, M. Calandra, and F. Mauri, *Nat. Phys.* **8**, 131 (2012).
- ¹¹R. Nandkishore, L. S. Levitov, and A. V. Chubukov, *Nat. Phys.* **8**, 158 (2012).
- ¹²B. Uchoa and A. H. Castro Neto, *Phys. Rev. Lett.* **98**, 146801 (2007).
- ¹³I. I. Mazin and A. V. Balatsky, *Philos. Magn. Lett.* **90**, 731 (2010).
- ¹⁴M. Q. Xue, G. F. Chen, H. X. Yang, Y. H. Zhu, D. M. Wang, J. B. He, and T. B. Cao, *J. Am. Chem. Soc.* **134**, 6536 (2012).
- ¹⁵P. N. First, W. A. de Heer, T. Seyller, C. Berger, J. A. Stroscio, and J.-S. Moon, *MRS Bull.* **35**, 296 (2010).
- ¹⁶P. Lauffer, V. Emtsev, R. Graupner, Th. Seyller, L. Ley, A. Reshanov, and B. Weber, *Phys. Rev. B* **77**, 155426 (2008).
- ¹⁷J. Hass, F. Varchon, J. E. Millán-Otoya, M. Sprinkle, N. Sharma, W. A. de Heer, C. Berger, P. N. First, L. Magaud, and E. H. Conrad, *Phys. Rev. Lett.* **100**, 125504 (2008).
- ¹⁸N. Emery, C. Hérodol, M. d'Astuto, V. Garcia, Ch. Bellin, J. F. Maréché, P. Lagrange, and G. Loupias, *Phys. Rev. Lett.* **95**, 087003 (2005).
- ¹⁹G. F. Sun, J. F. Jia, Q. K. Xue, and L. Li, *Nanotechnology* **20**, 355701 (2009).
- ²⁰Z. H. Ni, W. Chen, X. F. Fan, J. L. Kuo, T. Yu, A. T. S. Wee, and Z. X. Shen, *Phys. Rev. B* **77**, 115416 (2008).
- ²¹C. Faugeras, A. Nerrière, M. Potemski, A. Mahmood, E. Dujardin, C. Berger, and W. A. de Heer, *Appl. Phys. Lett.* **92**, 011914 (2008).